Amino Acid Residues of Leishmania donovani Cyclophilin Key to Interaction with Its Adenosine Kinase: Biological Implications †

ARTICLE *in* BIOCHEMISTRY · AUGUST 2007

Impact Factor: 3.02 · DOI: 10.1021/bi602625h · Source: PubMed

7 AUTHORS, INCLUDING:

Banibrata Sen
University of Texas MD Anderson Cancer Center
28 PUBLICATIONS **413** CITATIONS
SEE PROFILE

Venu Vandavasi
Oak Ridge National Laboratory
8 PUBLICATIONS **49** CITATIONS
SEE PROFILE

Subhankar Dolai
University of Toronto
17 PUBLICATIONS **252** CITATIONS
SEE PROFILE

Rahul Banerjee
Saha Institute of Nuclear Physics
38 PUBLICATIONS **694** CITATIONS
SEE PROFILE

Amino Acid Residues of *Leishmania donovani* Cyclophilin Key to Interaction with Its Adenosine Kinase: Biological Implications†

Banibrata Sen,‡ V. Venugopal,§ Anutosh Chakraborty,‡,|| Rupak Datta,‡,⊥ Subhankar Dolai,‡ Rahul Banerjee,§ and Alok K. Datta*,‡

The Division of Structural Biology and Bioinformatics, Indian Institute of Chemical Biology, 4, Raja S. C. Mullick Road, Kolkata-700032, India, and Crystallography and Molecular Biology Division, Saha Institute of Nuclear Physics, 1/AF Bidhannagar, Kolkata-700064, India

Received December 21, 2006; Revised Manuscript Received April 26, 2007

ABSTRACT: Cyclophilins (CyPs), by interacting with a variety of proteins, often modulate their biological activities and thus have been implicated in several cellular functions. However, mechanisms that determine such interactions are poorly understood. We earlier reported that an endoplasmic reticulum (ER)-located cyclophilin (LdCyP) from the purine auxotrophic parasitic protozoan *Leishmania donovani* reactivated its adenosine kinase (AdK). The AdK-reactivating property of LdCyP was however abolished at high ionic strength but not by nonionic detergents. Modeling of LdCyP, based on its crystal structure solved at 1.97 Å resolution, revealed several solvent-exposed hydrophobic and charged residues. Mutagenesis of several of such solvent-exposed residues was performed and their corresponding activities with regard to their (i) AdK reactivation property, (ii) ability to form complex with the enzyme, (iii) capacity to induce red shift in the intrinsic tryptophan fluorescence maxima of AdK, and (iv) efficiency to withdraw the ADP inhibition from the AdK-mediated reaction were compared to the wild-type protein. Results indicated that while the replacement of R147 with either A or D severely impaired all of the above characteristics displayed by the wild-type LdCyP, the effect of mutating K114 and K153 was although relatively less but nevertheless noticeable. Alteration of other exposed hydrophobic and charged residues apparently did not have any discernible effect. Under the condition of cellular stress, the ER-located LdCyP is released into the cytoplasm with concomitant increase both in the specific activity of the cytosol-resident AdK and the uptake of radiolabeled Ado into the cells. These experiments, besides demonstrating the importance of the positive charge, identified R147 as the most crucial residue in the LdCyP−AdK interaction and provide evidence for the stress-induced retrograde translocation of LdCyP from the ER to the cytoplasm. A possible implication of this interaction in the life cycle of the parasite is proposed.

Cyclophilins (CyPs),[1] besides mediating the cyclosporin A (CsA)-induced immunosuppression, also participate in various cellular processes ranging from cell division, receptor maturation, protein folding and its export, and protection against human immunodeficiency virus (HIV) infection to several other important cellular steps (*1*−*10*). Activities of various enzymes, transcription factors, and heat shock proteins have also been shown to be modulated by binding with CyPs (*11*−*14*). Sequence comparison of CyPs from various sources, all of which carry an associated peptidyl−prolyl *cis*−*trans* isomerase (PPIase) activity, revealed the presence of a central core domain consisting of a consensus CsA binding motif and a predominance of ionic residues at the C-terminal end (*15*). In most cases, the C-terminus of PPIase has been implicated in chaperone activity (*16*). Moreover, localization of various isoforms of CyPs in different cellular organelles has revealed several subtleties with regard to their biological functions (*17*).

Purine auxotrophic parasitic protozoon, *Leishmania donovani*, goes through a dimorphic life cycle. In the alimentary tract of the sandfly, its insect vector, the parasite exists extracellularly as the motile promastigote, whereas in the phagolysosomal system of mammalian macrophages, it exists intracellularly as the nonmotile amastigote (*18*). During transformation from one stage to the other, the activity levels of a large number of proteins are known to be stage-specifically altered either due to increased transcription or by other presently unknown mechanisms (*19*, *20*). Adenosine kinase (AdK), due to its ability to phosphorylate a large

† This work was initially supported by grants from the Department of Science & Technology (SP/SO/D-38/2000) and the CSIR Network Project (SMM003), Government of India. Presently, A.K.D. is an Emeritus Scientist of the Council of Scientific and Industrial Research, Government of India. B.S., V.V., and S.D. were supported by individual fellowships from the Council of Scientific & Industrial Research, Government of India.

* Address correspondence to this author. Tel: +9133-2473-6793/0492. Fax: +9133-2473-5197. E-mail: alokdatta@iicb.res.in.

‡ Indian Institute of Chemical Biology.

§ Saha Institute of Nuclear Physics.

|| Present address: Department of Neuroscience, Johns Hopkins University School of Medicine, 725 North Wolfe St., Baltimore, MD 21205.

⊥ Present address: Department of Biochemistry and Molecular Biology. St. Louis University School of Medicine, St. Louis, MO 63104.

[1] Abbreviations: DTT, dithiothreitol; AdK, adenosine kinase; CsA, cyclosporin A; LdCyP, *Leishmania donovani* cyclophilin; CyP, cyclophilin; Ado, adenosine; DSS, disuccinimidyl suberate; AMP, adenosine 5′-monophosphate.

10.1021/bi602625h CCC: $37.00
Published on Web 06/07/2007

variety of potentially pharmacologically active nucleoside analogues, is considered as one of the prospective purine salvage enzymes for chemotherapeutic manipulation. It has been demonstrated that the differential pattern of Ado utilization between the intracellular amastigote and extracellular promastigote forms is accompanied with a marked increase in the specific activity of AdK in the amastigote stage (*21*). However, to date there is no evidence to suggest that the higher activity is due to increased protein synthesis. Since AdK plays a major role in the metabolism and uptake of Ado, a key modulator of various cellular functions, the stage-specific activity of the enzyme may be relevant in the context of the life cycle of this purine auxotrophic parasite.

Unlike multidomain CyP (CyP40) and FK506 binding proteins, many single-domain CyPs (CyPA, CyPB, CyPC and ninaA etc) do not harbor the core tetratricopeptide (TPR) domain (*22*). Yet, they are known to bind a large number of proteins (*4*, *10*−*14*). It was recently found that *L. donovani* AdK, which shows progressive decrease in its reaction rate during extended periods of reaction, could be reactivated when near stoichiometric amount of LdCyP was present in the reaction mixture (*23*, *24*). This effect, exerted instantaneously, shows isomerase independence and also occurs under simulated *in vivo* conditions where AdK was allowed to coexpress with LdCyP, thereby indicating the interaction to be quite specific (*25*). However, unlike other chaperone−protein interactions, the LdCyP−AdK association appears to be weak and could be detected only in the presence of protein cross-linkers (*24*, *26*−*30*). Further *in vitro* studies indicated that (i) ADP, one of the products of the reaction, induced aggregation of the enzyme resulting in its inactivation and (ii) LdCyP, by interacting with AdK, disaggregated the enzyme by competing out the ADP, resulting in withdrawal of inhibition caused by ADP-mediated aggregation. This is reflected in reactivation of the enzyme (*23*). Clearly, therefore, the mechanism by which LdCyP reactivates AdK is unique and differs from other single-domain CyP−protein interactions (*4*, *10*, *31*). Despite all of these indications, very little is known regarding the mechanism of interaction and specific determinant(s) that dictate the binding specificity of this single-domain LdCyP toward AdK or for that matter any CyP−protein interactions, in general.

Another aspect of the present work involves studies related to the biological implication of this interaction. Unlike other organisms, *L. donovani* appears to lack a CyP-like protein in its cytoplasm (*32*). The only CyP-like activity (LdCyP) that has been shown to be present in this parasite is localized in the endoplasmic reticulum (ER) (*32*). On the contrary, AdK is strictly a cytosolic enzyme, thus raising a question about the physiological feasibility of this interaction.

To provide answers to the above queries, we have adapted the structure-guided site-specific mutagenesis approach to identify the amino acid residues of LdCyP involved in binding to AdK. The results show that surface-exposed hydrophobic residues of LdCyP exert the least influence on the binding and reactivation of the enzyme. Likewise, acidic residues also did not have a detectable effect. In contrast, mutation of some of the solvent-exposed positively charged amino acid residues resulted in dramatic loss of activity. The results also indicated that, under the condition of cellular stress, the specific activity of the cytosol-located AdK showed marked increase with concomitant enhancement in the rate of formation of intracellular AMP. Concomitantly, the ER-located LdCyP was found to be released into the cytoplasm, thus providing first-hand evidence of retrograde translocation of LdCyP from the ER to the cytoplasm and implicating its possible role in enzyme regulation during transformation.

MATERIALS AND METHODS

Materials. Unless otherwise stated, all of the chemicals were of analytical grade and were obtained from Sigma Chemicals.

Site-Directed Mutagenesis. All mutations were carried out using Stratagene's Quickchange site-directed mutagenesis kit. Wild-type LdCyP harbors only one essential "Trp" residue at position 122 that constitutes one of the amino acids of its consensus CsA-binding motif (WLDGRHVVFG) (*32*, *33*). Since the LdCyP-mediated chaperone function described here is CsA-independent, the W122 was mutated to G. The resulting mutant (mLdCyP), despite the loss of its fluorescence emitting property, was equally efficient in reactivating AdK and therefore turned out to be an excellent reagent for studying fluorescence emission characteristics of the client protein (AdK) during its interaction with LdCyP (*23*). Because of this advantage, unless otherwise stated, most of the mutations were carried out on the mLdCyP DNA template cloned in the N-terminal $(His)_6$-tagged expression plasmid (pQE32). The following sense primers, with their substitution sites underlined, along with their antisense counterpart were used: K99L, 5′-GGGACGGGCGGC**CTG**TCGATCTACGGC-3′; K105I, 5′-GTCGATCTACGGCGAA**ATC**TTCGCGGACGAGAAC-3′; E109L, 5′-GGCGAAAAGTTCGCGGAC**CTG**AACTTGAACGTAAAACAC-3′; K114M, 5′-GACGAGAACTTGAAGCTA**ATG**CACTTTGTGGGTGCGCTG-3′; K114R, 5′-CGAGAACTTGAAGCTA**AGA**CACTTTGTGGGTGCGC-3′; K114D, 5′-GACGAGAACTTGAAGCTA**GAC**CACTTTGTGGGTGCGCTG-3′; R147A, 5′-CCGTGGCTTGATGGC**GCC**CATGTGGTTTTCGGC-3′; R147D, 5′-CCGTGGCTTGATGGC**GAC**CATGTGGTTTTCGGC-3′; R147K, 5′-CGCCGTGGCTTGATGGC**AAG**CATGTGGTTTTCGGC-3′; K153M, 5′-CATGTGGTTTTCGGC**ATG**GTGCTTGATGGTATGC-3′; K153R, 5′-CATGTGGTTTTCGGC**CGG**GTGCTTGATGGTATGC-3′; K153D, 5′-CATGTGGTTTTCGGC**GAC**GTGCTTGATGGTATGC-3′; D159V, 5′-GCTTGATGGTATG**GTC**GTGGTCGTCCGC-3′; R163A, 5′-GGACGTGGTCGTC**GCC**ATCGAGAAGACAAAGAC-3′; K168M, 5′-CGCATCGAGAAGACA**ATG**ACGAACAGCCACGATCGC-3′; R174A, 5′-ACGAACAGCCACGAT**GCC**CCGGTGAAGCCC-3′; K177M, 5′-CACGATCGCCCGGTG**ATG**CCCGTGAAGATCG-3′; K177R, 5′-CGATCGCCCGGTG**CGG**CCCGTGAAGATCG-3′; F93G, 5′-GACTTCACCAAC**GGC**GATGGCACGGGC-3′; Y102N, 5′-GGCGGCAAGTCGATC**AAC**GGCGAAAAGTTCGCGGAC-3′; F90G, 5′-CAGGGCGGCGAC**GGC**ACCAACTTCGATGGC-3′. Mutations were confirmed by automated DNA sequencing in a Perkin-Elmer ABI Prism-DNA sequencer.

Expression and Purification of Proteins. Detailed methods of expression and purification of wild type and its various mutant forms of LdCyP and AdK have been published elsewhere (*23*, *24*, *34*). Detailed CD analysis of the mutant proteins failed to detect any change in their structures (data not shown).

AdK Reactivation Assay. The reactivation of AdK was monitored under saturating substrate concentration using the radiochemical assay procedure as described earlier (*23*, *24*, *34*, *35*). Wherever indicated, wild-type and mutant LdCyPs, KCl, NH_4Cl, and various detergents were included as per requirement of the respective experiments. Unless stated, all of the assays were performed at 30 °C for 30 min. For product inhibition studies with ADP, assays were performed for 15 min at 30 °C in the presence of 400 μM ATP as described previously (*23*).

Cross-Linking Studies. DSS-mediated cross-linking of AdK (10 μM) with either wild type or different mutants of LdCyP (10 and 30 μM) was carried out following earlier methodology (*24*). The separated protein bands were visualized following immunoblotting with rabbit polyclonal antiserum raised against AdK.

Fluorescence Measurement. Intrinsic tryptophan fluorescence of AdK was monitored using a Hitachi F-4500 spectrofluorometer as described in previous reports (*23*, *25*). Briefly, to study the influence of LdCyP on the emission property of Trp fluorescence of AdK, the nonfluorescent mLdCyP and its R147A mutant form were used, wherever indicated. The buffer contained 20 mM Tris-HCl (pH 7.5) and 1 mM DTT. The concentration of AdK was 1 μM. The concentrations of mLdCyP and its R147A form were maintained at 2 μM each.

Subcellular Fractionation. L. donovani (UR6) promastigotes were grown in solid blood−agar media as described elsewhere (*36*). Cells, harvested from the late logarithmic culture, were washed twice by centrifugation at 1200*g* (4 °C) for 15 min in HBSS with sodium bicarbonate, pH 7.2 (University of Iowa Cancer Center). Promastigotes were then resuspended in 500 mL of HBSS at a cell count of 5×10^9/mL. Baseline viability was quantified microscopically according to flagellar motility by grading a minimum of 200 promastigotes as motile (viable) or nonmotile (nonviable). To mimic the mammalian macrophage environment, *L. donovani* cells were grown in HBSS at 37 °C alone or in conjunction with 75 μM H_2O_2 (sublethal concentration) (*37*−*39*). Parasites grown at 26 °C in HBSS served as the control. The following procedures were performed at 4 °C for subcellular fractionation. Cells grown under different conditions were centrifuged and washed twice in STE buffer (0.32 M sucrose, 25 mM Tris-HCl, and 1 mM EDTA, pH 7.8). Pelleted cells were mixed with silicon carbide to form a paste and disrupted by grinding with a pestle and mortar (*40*, *41*). Grinding was continued until 90% of the cells were lysed as viewed by phase-contrast microscopy. The suspension was diluted 5−10-fold in STE buffer and briefly centrifuged for 3 min at 100*g*. The pellet was washed once in STE buffer and centrifuged. The combined supernatants were centrifuged for 10 min at 1000*g* to remove nuclei and unbroken cells. The resultant supernatant was then centrifuged at 14500*g* for 10 min. The pellet obtained contained the large granular fraction. The supernatant was spun for 1 h at 139000*g*. The resulting supernatant was the cytosolic fraction. The pellet dissolved in the STE buffer contained small granules termed as the microsomal fraction. Microsomal (50 μg) and cytosolic (500 μg) fractions of each culture were then subjected to SDS−PAGE (13%) and analyzed by western blotting using LdCyP, AdK, and anti-calreticulin (BD Bioscience) polyclonal antisera.

[^{3}H]Ado Incorporation Studies. To determine intracellular AMP formation, late logarithmically grown *L. donovani* cells were harvested, washed twice with ice-cold 1× PBS, and resuspended in HBSS buffer (4×10^7 cells/mL) lacking purines (*42*). The incorporation experiment was performed with three different sets (0.9 mL each) of cell suspensions. The first set of cell suspension was incubated at 26 °C as the control while the other two sets were exposed to 37 °C either in the absence or in the presence of H_2O_2 (75 μM) as the oxidizing agent (*43*). After 1 h of incubation under this condition, [^{3}H]Ado (2000 cpm/pmol, 20 μM) along with inosine and adenine was added to the cell suspension at final concentrations of 5 μM, 0.1 mM, and 0.1 mM, respectively (*42*). In *L. donovani*, the metabolism of Ado can take place by three different routes (*21*). In the first pathway, Ado can be directly phosphorylated to AMP by AdK, whereas in second and third pathways, Ado can either be deaminated to inosine by adenosine deaminase present in the amastigotes or be converted to adenine by adenase, present exclusively in the promastigote stage of the life cycle (*21*). Therefore, inclusion of inosine and adenine in the reaction mixture minimized the extent of conversion of [^{3}H]Ado to inosine and adenine via adenosine deaminase and adenase pathways, respectively, if any (*42*). At indicated time intervals, cell suspension (0.2 mL) from each set was removed and placed on a boiling water bath. After sonication in presence of Triton X-100 (10%), all of the suspensions were centrifuged. Aliquots (50 μL) were withdrawn from the clarified supernatant and assayed for AMP formation after spotting on DE-81 paper as described previously (*25*).

Immunodepletion Experiment. Immunoprecipitation of LdCyP from the cytosolic extracts of unstressed and stressed cells was carried out as follows. Initially, preswelled protein A−Sepharose CL-4B was incubated separately with either preimmuned sera or LdCyP-polyclonal antisera at room temperature for 3 h. Using ice-cold 1× PBS (pH 7.5), the unadsorbed protein was thoroughly washed off from the beads. To each cytosolic extract (200 μg), as indicated, 75 μL of the antibody-conjugated protein A−Sepharose CL-4B (an equivalence for rabbit γ-globulin in order to facilitate immunoprecipitation) suspension was added and kept for an additional 1 h at 30 °C followed by 30 min in ice. As control, treatment of the extracts with preimmuned sera-treated protein A−Sepharose 4B was also carried out simultaneously. All of the mixtures were centrifuged, and the supernatants obtained were assayed for enzymatic activity using the standard assay condition or for immunoblotting.

Modeling Studies. The crystallization and low-resolution structure of LdCyP has already been reported (*44*). The high-resolution crystal structure of LdCyP was solved by molecular replacement (AMoRe) using the homologous molecule from *Trypanosoma cruzi* (PDB code 1xo7) as the search model (*45*). Subsequently, the three-dimensional model was built on a Silicon Graphics workstation utilizing the O software and refined using CNS (*46*, *47*). Several cycles of alternating manual model building and refinement led to the final high-resolution crystal structure of 1.97 Å with an R and R_{free} of 0.178 and 0.197, respectively. The model was validated by PROCHECK and exhibted no residues in disallowed regions of the Ramachandran plot (*48*). The rms deviations in bond lengths and bond angles were 0.007 Å and 1.40°, respectively. Although the details of the high-

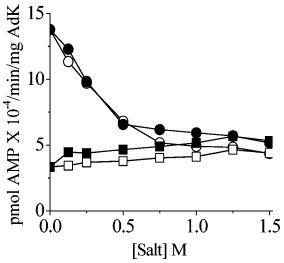

FIGURE 1: LdCyP reactivation of AdK as a function of ionic strength. The enzyme (50 nM) in the presence (●, ○) or in the absence (□, ■) of CyP (5 μM) was assayed in the presence of increasing KCl (○, □) and NH_4Cl (●, ■) concentrations.

resolution crystal structure will be reported elsewhere (manuscript in preparation), the coordinates have been deposited in the Protein Data Bank (PDB code 2haq). The mutant models were generated by the MODELLER software using the coordinates of 2haq as the template (*49*). The buried residues were determined by calculating their "solvent-accessible area" (SAA) in the protein and computing their ratios with SAA of the same amino acid (X) in a Gly-X-Gly tripeptide (*50*, *51*). Residues with a ratio less than 0.05 were considered as completely buried. The electrostatic surfaces of the models were calculated using GRASP with a color range from −18.0*kT* (red) to +18.0*kT* (blue) (*29*).

RESULTS

AdK Reactivation Is Salt but Not Detergent Sensitive. To investigate the nature of the interaction, the LdCyP-mediated AdK reactivation assay was performed in the presence increasing concentrations of monovalent salts and different nonionic detergents, used at concentrations (1−2%) sufficient to inhibit interaction between some but not all proteins (*52*, *53*). Results showed that LdCyP-mediated AdK reactivation remained unaffected in the presence of a battery of nonionic detergents. Sorbitol and glycerol also did not have any effect (data not shown). Surprisingly however, salt, which as such did not have any discernible effects on the activity of the enzyme as measured by our assay system, completely abolished the LdCyP-mediated reactivation of AdK (Figure 1). The extent of inhibition of the LdCyP-stimulated activity, which was initially directly proportional to the concentration of the salt, reached a plateau level that corresponded with the activity displayed by the enzyme in the absence of LdCyP. Additional salt failed to augment any further inhibition. These results indicated that the reactivation of AdK which resulted due to its interaction with LdCyP was sensitive to high ionic strength, a finding consistent with many other reports (*52*, *54*, *55*).

Selection of Interacting Residues of LdCyP Based on Its Crystal Structure. Beside ionic interaction, several other interacting forces are known to be involved in stabilizing protein−protein recognition (*56*). However, in view of the results of the preceding section, it appeared that ionic residues probably play an important role in the interaction. In order to determine how much contribution the charge makes over other forces in this particular interaction, an algorithm was designed to identify the exact amino acids directly involved in the binding. Several experimental observations guided the procedure: (i) the availability of the high-resolution (1.97 Å) LdCyP crystal structure (PDB accession code 2haq),

Table 1: Fraction of Surface Accessibility of Putative Interacting Residues of Cyclophilin Based on the Crystal Structure of the Molecule[a]

	burial profile of selected residues in full-length cyclophilin	
residue	SAA	fraction of SAA exposed
F90	26.59	0.13
F93	95.48	0.47
K99	88.66	0.40
Y102	98.28	0.42
K105	94.15	0.42
E109	60.84	0.31
K114	147.43	0.66
R147	142.56	0.56
K153	64.46	0.30
R163	127.98	0.50
K168	156.18	0.70
R174	128.74	0.50
K177	93.32	0.42

[a] SAA represents the solvent-accessible area (probe radius 1.4 Å) of individual amino acids based on crystal structure coordinates. Fraction of SAA exposed refers to the fraction of the solvent-accessible area exposed to the solvent in the three-dimensional structure relative to a completely exposed conformation (Gly-X-Gly fragment) of the same residue, calculated using the published method (*50*, *51*). Visual enumeration shows that residues with fraction of SAA >0.30 are predominantly exposed to the solvent.

which allowed inspection of the surface features of the protein, (ii) the high degree of sequence conservation of the binding site residues among CyPs from other sources (Figure 2), (iii) an earlier result demonstrating high potency of a truncated LdCyP, devoid of the first 88 amino acid residues from the N-terminus, in reactivating AdK (*24*), and (iv) the ability of mammalian CyPA to reactivate parasitic AdK and vice versa (data not presented). On the basis of these observations and the fraction of surface-accessible area (SAA) (≥0.25) exposed, several hydrophobic and charged residues (viz., F90, F93, K99, Y102, K105, E109, K114 R147, K153, D159, R163, K168, R174, and K177), located especially at the C-terminal end of the protein, were selected and targeted for mutagenesis (Table 1). The LdCyP mutants were expressed in *Escherichia coli*, purified, and tested for their (i) AdK reactivation property, (ii) ability to form a complex with the enzyme, (iii) ability to induce a red shift of the intrinsic tryptophan fluorescence maxima of AdK, and (iv) efficiency to withdraw the ADP inhibition from the AdK-mediated reaction.

R147 → A or D Mutation Abrogates the AdK Reactivating Property of LdCyP. Following the reactivation assay, the extent of AdK stimulation as a function of chaperone concentration was monitored using various mutants of LdCyP. The reactivation assay indicated that substitution of hydrophobic residues (F90, F93, and Y102) with nonpolar glycine barely reduced the capacity of the respective mutant proteins to stimulate AdK. Similarly, mutation of several charged residues, viz., K99L, K105I, E109L, K99L/E109L double mutant, R163A, K168M, and R174A, failed to show any significant reduction in AdK stimulating activity and were therefore excluded from subsequent experiments (data not shown). In contrast, alterations of R147 to A led to almost complete loss of its ability to reactivate AdK activity (Figure 3A). Mutant R147 → D also gave similar results (Figure 3A). However, K114 to M and K153 to M mutations of

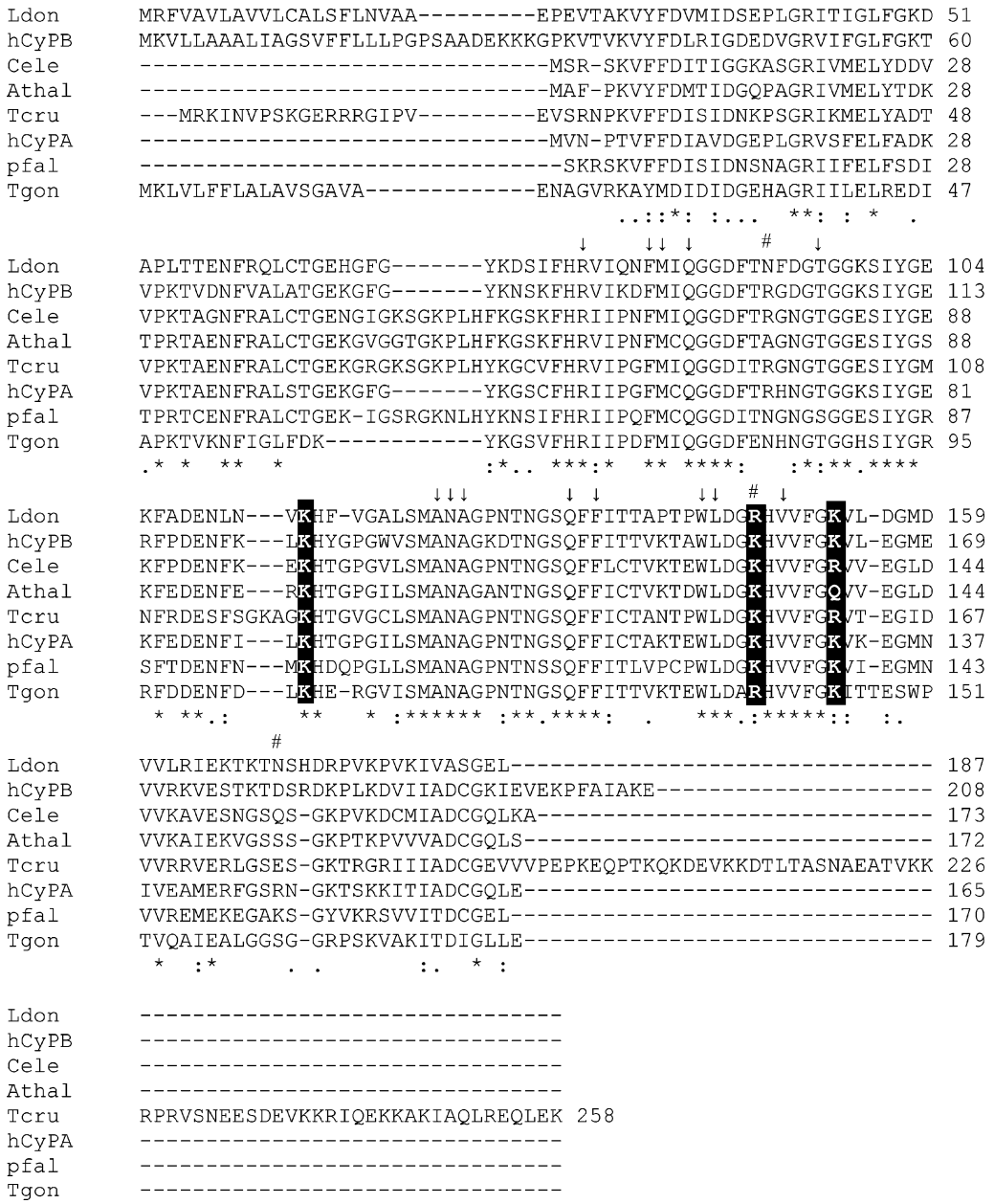

FIGURE 2: Comparison of the predicted amino acid sequence of LdCyP (accession no. AAD46565) with CyPs from human CyPA (accession no. 1CWLA), human CyPB (accession no. AAA52150), *Caenorhabditis elegans* (accession no. P52011), *Arabidopsis thalliana* (accession no. P34790), *T. cruzi* (accession no. O76990), *P. falciparum* (accession no. 1QNGA), and *T. gondii* (accession no. AAA17997). The sequences were aligned by the CLUSTAL W program. Amino acid residues predicted to be involved in CsA binding and calcineurin docking are represented by (↓) and (#), respectively. Amino acids indicated by dark boxes are the probable targets of AdK docking.

LdCyP led to somewhat variable degrees of reduction in the AdK-stimulating property in comparison to the wild-type LdCyP (Figure 3A). Mutant K114 → D and K153 → D proteins also were partially inactive (data not shown). In this context it needs to be pointed out that, in CyPs from many other sources, the amino acid equivalent of R147 of LdCyP is replaced with K (Figure 2). It was therefore of interest to investigate whether the AdK-stimulating activity displayed by LdCyP is R147 specific. To determine this, the inactive R147A mutant was remutagenized to R147K. Interestingly, the R147K mutant protein became as active as the wild-type LdCyP in stimulating AdK (Figure 3B). Likewise, the AdK-stimulating abilities of K114R and K153R mutants also improved to a large extent over K114M and K153M mutants (Figure 3B).

The observed stimulatory effect of the wild type and R147K mutant was discernible regardless of whether the reaction mixture contained the respective chaperones from the beginning of the reaction or was added at later times during the progression of the reaction. However, the R147A mutant was inactive under both circumstances (Figure 3C). Collectively, these results are consistent with the interpretation that whereas the positive charge on the residue 147 is essential, the positive charges on residues K114 and K153 appear to play some sort of supportive roles in the reactivation process.

The Electropositive Character of "Residue 147" Is Crucial for Complex Formation. Since a direct contact between AdK and LdCyP is a prerequisite for reactivation, the loss of the reactivating property of some of these mutant LdCyPs could

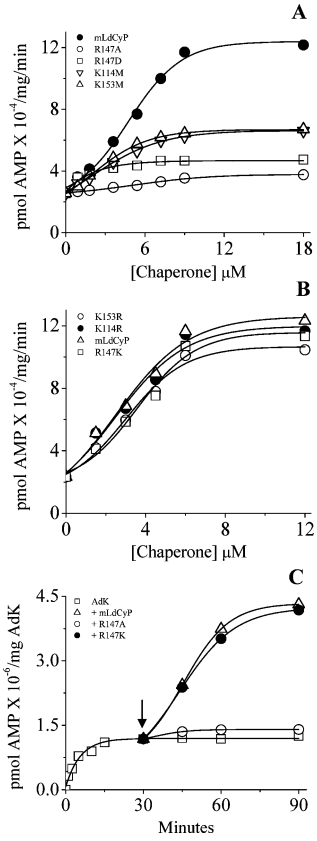

FIGURE 3: Surface positive charges of LdCyP are indispensable for the reactivation process of AdK. The activity of the enzyme AdK (50 nM) was monitored in the presence of indicated concentrations of the wild-type and various mutant proteins from the beginning of the reaction (A and B). Reactivation of AdK was carried out in the presence of mutant LdCyP, where the positively charged residue was substituted with either nonpolar hydrophobic residues or acidic residues (A) and with other corresponding basic amino acids (B), whereas in the results depicted in (C), the wild type and mutant chaperone were added after 30 min (indicated by ↓) of AdK reaction without it. Corresponding symbols were explained in the respective figure.

be due to (i) lack of interaction between the two proteins, (ii) loss of chaperone function of these mutant CyPs despite proper interaction, or (iii) loss of both of the properties. In order to determine the mechanism that limits the process, AdK was allowed to interact with various mutants of LdCyP in the presence of the protein cross-linker, DSS (*24*, *25*). From the results it is clear that the inactive R147A mutant, unlike the wild-type LdCyP, failed to form the DSS-mediated AdK−LdCyP adduct (∼56 kDa), an established indication of complex formation between the two proteins (Figure 4, lanes 5 and 6) (*24*, *25*). However, the same band could be immediately visualized when R147K, instead of R147A, was used to interact with AdK (lane 7). In contrast, mutant R147D, which failed to stimulate the enzyme activity, also could not form the adduct (lanes 8 and 9). Similarly, K114M and K153M proteins, which failed to stimulate AdK as efficiently as the wild type or the R147K mutant, were unable to form a complex with AdK (data not presented). Another notable aspect is the observation that adduct (∼56 kDa band) formation was invariably associated with a concomitant increase in the extent of disaggregation of the protein, as evident from the accumulation of increased amounts of protein at a position corresponding to monomeric size of AdK (38 kDa). Taken together, these results support the

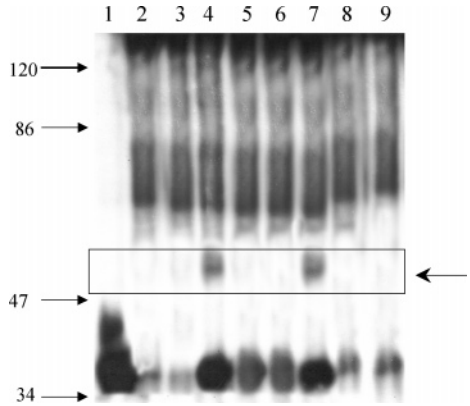

FIGURE 4: Comparative ability to cross-link AdK with wild type and various mutants of LdCyP provides the evidence of direct interaction. AdK (10 μM) was incubated with DSS in the presence of wild-type LdCyP and its various mutants. Lane 1 shows control AdK without DSS, lanes 2 and 3 indicate AdK with DSS, lanes 4−9, in order, indicate AdK with wild-type LdCyP (10 μM), R147A (15 μM), R147A (30 μM), R147K (10 μM), R147D (15 μM), and R147D (30 μM), respectively. The arrow indicates the ∼56 kDa band corresponds to the LdCyP-AdK adduct. For details, refer to Materials and Methods.

interpretation that while the positive charge on the residue 147 is crucial and forms the nucleus of binding, K114 and K153 possibly play a supporting role in stabilization of the binding.

The R147A Mutant Fails To Induce Conformational Modulation of AdK, Thereby Preventing Withdrawal of ADP Inhibition. By using the "mLdCyP-mediated tryptophan fluorescence red shift of AdK" as an assay system, it has recently been shown that LdCyP induces some sort of conformational reorientation of AdK, resulting in reduced affinity of the enzyme toward ADP with consequent relief of the enzyme from its own product-mediated inhibition (*23*). In the present experiment it is shown that AdK, in the presence of mLdCyP, showed a distinct red shift in its fluorescence maxima (Figure 5A, curve 2). However, the R147A mutant of mLdCyP failed to induce such an effect on the AdK (Figure 5A, curve 3). The inability of the R147A mutant to induce such a red shift is also reflected in its reduced efficiency to withdraw ADP inhibition from the AdK-mediated reaction (Figure 5B). In contrast, the behavior of R147K was similar to mLdCyP in terms of both of these properties, thereby providing support to the interpretation that loss of the AdK-reactivating property of R147A LdCyP was clearly due to its inability to bind to AdK, a step prerequisite for the subsequent conformational reorientation of the AdK molecule. Stern−Volmer analysis of the interaction, often utilized for studying such binding properties, between AdK and LdCyP or its R147A mutant in the presence of small-molecule quenchers, KI and acryamide, also provided additional support to such an interpretation (Figure 6).

Stress Induces Dislocation of the ER-Located LdCyP into the Cytoplasm. As opposed to AdK which is located exclusively in the cytoplasm, LdCyP is sequestered in the ER of the parasite (*32*). Moreover, despite extensive efforts no CyP-like protein has yet been detected in the cytoplasm of *L. donovani* (*32*). Thus the biological function of this interaction becomes questionable. However, there are reports from several laboratories indicating that CyP, like Hsp70, is

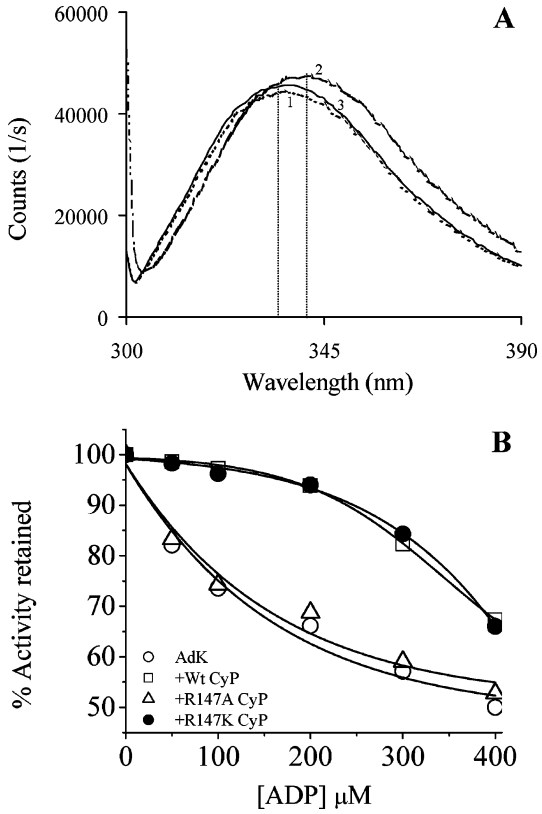

FIGURE 5: Mutant (R147A) LdCyP fails to induce conformational modulation of AdK and withdraw ADP inhibition from the AdK reaction as well. (A) The fluorescence emission spectra of AdK (1 μM) were monitored in the absence (curve *1*) and in the presence of 2 μM mLdCyP (curve 2) and R147A (curve 3) proteins, respectively. Excitation was performed at 295 nm. The excitation and emission slit length was set at 5 nm in each case. (B) The observed inhibition of AdK by ADP (○) was reassessed in the presence of wild-type (□), R147A (△), and R147K (●) LdCyP proteins. The concentration of the chaperone was maintained at 5 μM.

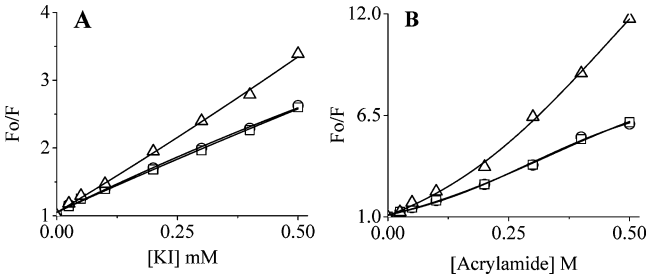

FIGURE 6: Comparison of Stern−Volmer plots of fluorescence quenching of AdK (□) by KI (A) and acryamide (B) in the presence of mLdCyP (△) and R147A (○) LdCyP.

indeed induced in various organisms when exposed to heat or other environmental shocks (*57*−*59*). Since *L. donovani*, during transformation from its extracellular promastigote form to the intracellular amastigote, faces a hostile environment of the macrophage consisting of acidic pH, high temperature, and oxidative stress, it was of interest to investigate the status of CyP in the parasite under stressed condition (*60*). With this end in view, we exposed late logarithmically grown cells at high temperature (37 °C) in the absence or in the presence of H_2O_2 that is known to mimic the condition inside the macrophage (*37*−*39*). The concentration of H_2O_2 was chosen in such a manner to avoid the killing of the parasite (*38*). Following the treatment, these cells, unlike the normal cells, looked rounded under the microscope but were nevertheless motile (not shown). Cellular subfractionation of both treated and untreated cells and immunoblot analysis of cytosolic and microsomal extracts from these cells with polyclonal LdCyP antibodies clearly indicated that the treated cells did not show any increase in the content of the existing LdCyP (Figure 7). Moreover, there was the appearance of hardly any other new additional LdCyP−antibody reactive proteins on the immunoblot. In this connection it should be pointed out that, due to the antigenic commonality among various isoforms of CyPs, the LdCyP−polyclonal antibody used in the present experiment was earlier shown to react with CyPs from various sources (*32*). Therefore, induction of any other additional CyP homologue, if at all any, should have been detected under this experimental condition. On the contrary, the experiment showed that LdCyP, which was located exclusively in the microsomal fraction of the untreated cells (Figure 7, panel A, lane 1), appeared in the cytoplasm of the treated cells (Figure 7, lanes 4 and 6). To rule out that this was not a generalized nonspecific phenomenon occurring due to damage of the cells or some other artifacts of cellular subfractionation, immunoblotting of these extracts was carried out with antibodies raised against AdK (38 kDa) and ER-anchored calreticulin (CR) (60 kDa) (*61*). The results showed that AdK (Figure 7, panel B, lanes 2, 4, and 6) and calreticulin (Figure 7, panel C, lanes 1, 3, and 5), as found in the untreated cells, remained localized to the cytoplasm and ER, respectively, in treated cells also. Moreover, the intensity of the AdK-specific band (Figure 7, panel B, lanes 2, 4, and 6) remained more or less same in both untreated and treated extracts, indicating no change in the level of the enzyme upon treatment. It is also to be noted that the molecular mass of the immunoreactive protein (17.8 kDa), detected in the cytoplasm of the stress-induced cells, corresponded with the size of the ER-located LdCyP and was significantly smaller (by ~2.9 kDa) than the size predicted from the open reading frame (*32*). Moreover, the same N-terminal sequence of the LdCyP (EPEVTAK) from both cytoplasmic and microsomal fractions of the stressed cells confirmed the identity of the two proteins. Therefore, the possibility that the appearance of the LdCyP in the cytoplasm could rather be due to stress-induced blockage of translocation of the nascent peptide from the cytoplasm to the ER can be ruled out. Taken together, the results are consistent with the interpretation that stress must be responsible for discharge of the LdCyP from the ER to the cytoplasm by a mechanism involving retrograde translocation. Such type of stress-induced dislocation of proteins has already been documented (*62*−*64*). The fact that LdCyP, even after discharge from the ER, remained equally active was confirmed when we observed higher specific activity of AdK in the cytosol of the treated cells in comparison to the cytosolic extract of the untreated cells, thus supporting the findings that unfolding is not a prerequisite for ER to cytosol dislocation (Figure 7, panel D) (*65*).

Stress Facilitates Increased AMP Synthesis in L. donovani. It is an established fact that AdK, because of its ability to phosphorylate Ado, provides the driving force for the uptake of Ado from the extracellular environment into the cell (*66*−*68*). Since cytoplasm-located AdK, despite its unchanged level, showed higher activity in the stressed *L. donovani* cells relative to its unstressed counterpart, it was of interest to

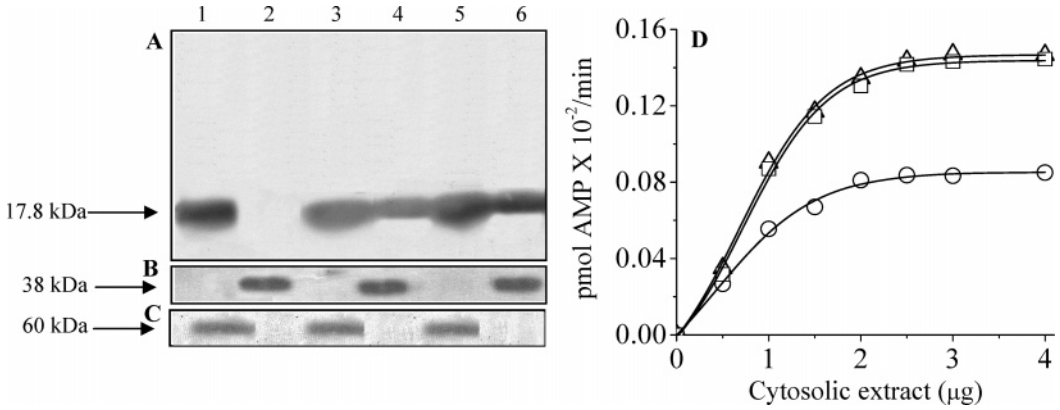

FIGURE 7: Stress induces dislocalization of LdCyP from the ER to the cytoplasm. Following cellular subfractionation, 50 μg of microsomal (lanes 1, 3, and 5) and 500 μg of cytoplasmic (lanes 2, 4, and 6) fractions from the normally grown (lanes 1 and 2), heat (lanes 3 and 4), and H_2O_2 + heat-exposed (lanes 5 and 6) *L. donovani* promastigotes were subjected to SDS−PAGE analysis and immunoblotted with polyclonal LdCyP (A), AdK (B), and calreticulin [CR] (C) antibodies. Panel D represents the levels of AdK activity present in the cytosolic extracts from these heat (□) and H_2O_2 + heat (△) treated cells being depicted and compared with the activity present in the normal cell cytosolic extract (○) with its increasing concentrations.

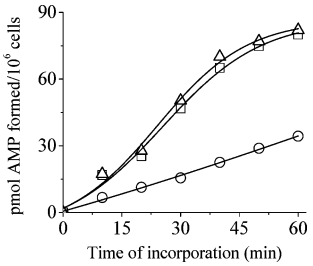

FIGURE 8: Kinetics of AMP formation in normally grown (○), heat (□), and H_2O_2 + heat (△) exposed *L. donovani* cells. Experimental details are in the Materials and Methods section.

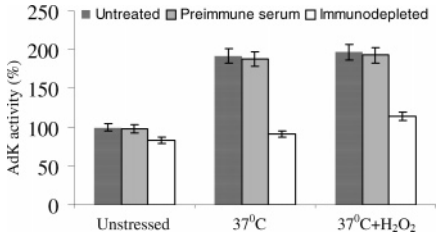

FIGURE 9: Activity of AdK in LdCyP-depleted cytosolic extracts of unstressed, heat stressed, and heat + oxidatively stressed *L. donovani* cells. The cytosolic extracts from the unstressed and stressed cells were subjected to treatment with LdCyP antibody-conjugated protein A−Sepharose 4B. Following immunoprecipitation of LdCyP, each extract was assayed for AdK activity. The control experiments without treatment and with preimmuned sera-conjugated protein A−Sepharose treated extracts were also carried out using the identical procedure. Activity displayed by the unstressed *L. donovani* cytosolic extract prior to immunodepletion was taken as 100%.

determine the status of AMP levels in both treated and untreated cells. In order to ascertain this, a [^{3}H]Ado incorporation experiment was carried out in both normal and stressed cells, and the level of [^{3}H]AMP was determined (Figure 8). The kinetics of [^{3}H]Ado incorporation indicated that the extent of AMP formed was indeed much higher in the stressed cells as compared to the normal cells. These results, when considered in conjunction with the concomitant release of ER-located LdCyP into the cytoplasm of the stressed cells, provide evidence in favor of LdCyP being probably responsible for the increased activity of the enzyme, resulting in an increased yield of AMP in the stressed cells (Figures 7 and 8). The relevance of this observation in relation to the biology of the parasite will be discussed in a subsequent section.

Immunodepletion of LdCyP Prevents AdK Reactivation. Levels of a wide variety of proteins are known to be altered upon exposure of *L. donovani* promastigotes to heat stress or treatment with hydrogen peroxide (*20*, *38*, *43*). Therefore, a question might arise as to whether the observed *in vivo* reactivation of AdK under stressed condition was due to the induction of some other heat-induced chaperonic proteins. In order to investigate such a possibility, the cytosolic extracts from both unstressed and stressed cells were depleted of LdCyP using LdCyP-antibodies bound to protein A−Sepharose 4B. Following immunodepletion, the extracts from each set were assayed for AdK activity under the identical condition. The results in Figure 9 clearly showed that, unlike the cytosolic extract obtained from the unstressed cells, the cytosolic extracts of the stressed cells following immunodepletion displayed lower levels AdK activity as compared to its corresponding untreated or preimmuned serum-treated extracts. Significantly, this low activity of these immunodepleted extracts corresponded with the activity level shown by the unstressed cytosolic extract. As expected, treatment with the preimmuned serum hardly had any effect on any of the extracts. These results clearly established that LdCyP dislocated into the cytoplasm of the stressed cells most likely was responsible for reactivation of the AdK activity.

DISCUSSION

Chaperones are usually defined by their ability to prevent aggregation of proteins following binding to its non-native early folding intermediates and assisting them in reaching their final native conformation (*69*). To this end, several chaperones have been reported of which CyP is considered as one of the candidates (*70*). During the past decade, a wide variety of cellular proteins have been shown to undergo specific association with CyPs (*1*−*10*, *12*−*14*). Despite this, there are presently only very few studies describing the biochemical mechanism of interaction of CyP with its client proteins (*71*). In the present work, deviating from the established notion of chaperone function, we describe a novel mechanism by which LdCyP reactivates an enzyme. Using

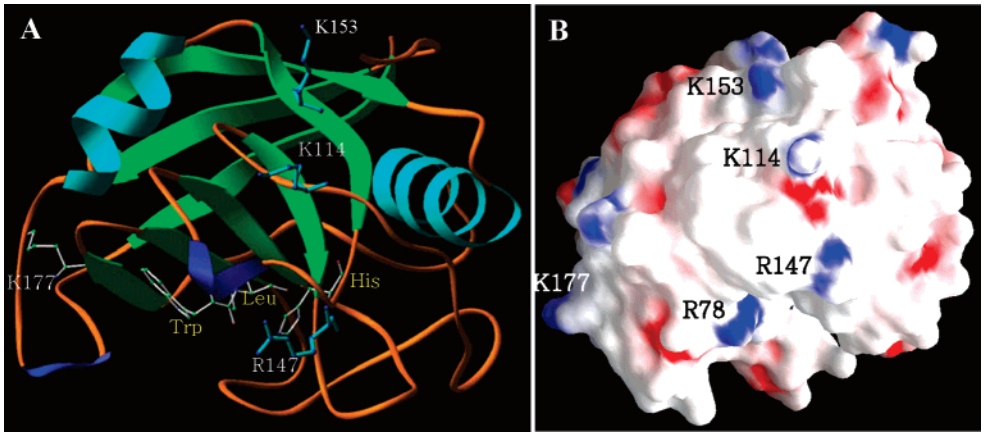

FIGURE 10: Spatial location of interacting residues on LdCyP in its native structure. (A) The ribbon diagram model, prepared using RIBBON, shows the relative positions of R147, K114, K153, and K177 relative to the CsA-binding residues Trp (W143), Leu (L144), and His (H148). The model is based on the coordinates calculated from the 1.97 Å crystal structure of LdCyP (PDB accession code 2haq). (B) Surface charge distribution of the modeled LdCyP was carried out using the procedure described in the Materials and Methods section. Negatively charged residues are in red, and positively charged residues are in blue. White represents both hydrophobic and neutral polar residues. Electrostatic surfaces were calculated using GRASP. The color range is from $-18.0kT$ (red) to $+18.0kT$ (blue).

AdK as the substrate protein, the molecular basis of LdCyP interaction with the enzyme has been studied, and the physiological significance of the interaction in the life cycle of the parasite has been probed.

The novelty of the present work lies in the identification of the residues (K114, R147, and K153) responsible for the interaction and providing evidence for the primary involvement of a specific amino acid (R147) in the process. These experiments although suggest that the interaction of LdCyP with AdK is guided primarily by electrostatic forces; it does not absolutely rule out that other interacting forces, viz., hydrophobic and mixed type, found in other chaperone−protein interactions, do not have any contribution in such process (*30*, *52*, *72*−*79*). It might be possible that the hydrophobic pocket of either of the proteins initially responsible for docking might get buried so much so following interaction resulting in nonaccessibility of even small nonionic detergent molecules. Notwithstanding the limitation of this information, since all three positively charged amino acids (K114, R147, and K153), located at the C-terminal end of the chaperonic protein, appeared to play important roles in the interaction, these results supported our previous findings as to why the truncated LdCyP, devoid of 88 amino acids from its N-terminal end, was still active in stimulating AdK (*24*).

The fact that electrostatic forces do play their part in orienting proteins during their functional binding to other proteins is well established (*80*). In a recent publication we demonstrated that the wild-type LdCyP, following interaction with AdK, induces some sort of subtle conformational alteration of the enzyme (*23*). This results in decreased affinity of the enzyme for one of its reaction product inhibitors, ADP, leading to ultimate relief from its inhibitory effect (*23*). This type of enzyme stimulatory mechanism by LdCyP is unique and is hitherto unknown in other chaperone-mediated reactions. In this connection, it will be interesting to note that the residue R147 of LdCyP or the equivalent lysine residue from other CyPs, that forms part of the consensus CsA-binding motif (WLDGK/RHVV), has been identified as one of the major residues involved in binding of calcineurin (*81*). On the contrary, the binding of *Toxoplasma gondii* CyP18 to the chemokine receptor CCR5, however, does not require this residue (*71*). These observations suggest that CyP binding to its various client proteins probably follows different mechanisms. Although much more extensive studies on such interactions involving a variety of CyPs from different sources and their client proteins will be needed to support this prediction, the fact that (i) human and *Plasmodium falciparum* CyPs, as opposed to *T. gondii* CyP18, do not display CCR5 binding activity and (ii) the four residues R90, K113, A128, and R158 of human CyPB, different from CyPA, exert a differential influence on calcineurin binding to these immunophilins supports such a contention (*82*, *83*).

Structural Specificity. The essentiality of positive charge on the "residue 147" of LdCyP in its interaction with its client protein AdK raises questions as to the structural characteristics determining such specificity. In order to probe this phenomenon, we modeled LdCyP based on the coordinates of its high-resolution crystal structure (PDB accession code 2haq). The ribbon diagram of the structure (Figure 10A) and the surface electrostatic potential map of the probable amino acid residues involved in the interaction (Figure 10B) clearly demonstrated that R147, one of the residues of the consensus CSA-binding motif (WLDGRHVV), protrudes out of the CsA-binding hydrophobic pocket. Furthermore, the R147 residue is definitely not involved in the binding of CsA (*81*). This validates the earlier observation as to why this unique chaperone function of LdCyP is isomerase independent. Surface charge representation further revealed that several other positively charged residues (R78, K114, K153, and K177) have considerably high surface exposure (Table 1). Of these, R78 was excluded from our studies due to its absence from the truncated LdCyP (N_{22-88}-DEL), which exhibits AdK-reactivating activity comparable to the full-length LdCyP (*24*). Similarly, the K177 residue appeared to be on the opposite face of the molecule (Figure 10B). Interestingly, K114 and K153 residues along with R147, which appear to play a major role in the interaction process, are arranged in a linear array and are surrounded by a large number of hydrophobic and neutral polar residues (Figure 10). These findings led us to postulate that a net positive electrostatic potential on this particular region of the LdCyP molecule, generated due to the presence of these three amino

acid residues, probably induces complementary negative electrostatic potential on the molecular surface of AdK, leading to reorientation of the molecule. Since the ADP-inhibition of AdK can be withdrawn by LdCyP, the most logical interpretation at this point would be that LdCyP binding to AdK modulates its conformation in a manner thereby facilitating ADP release (*23*). Future analysis of the surface residues of AdK would be essential to understand its specific interacting residues. In this context it will be worth mentioning that structural modulation and regulation of the ATP−ADP exchange rate of adenine nucleotide translocase are also controlled following binding of CyPD to the active site of the enzyme, a finding consistent with our proposal (*84*, *85*). The mechanism of the LdCyP−AdK interaction is to some extent analogous to the trigger factor (TF) binding to its client protein, where a net positive charge spread across a stretch of eight amino acids comprising of basic and aromatic residues was shown to influence the binding (*27*).

Relevance of the Interaction in Relation to Stimulation. There is increasing evidence suggesting that, in order to survive under stressful conditions, organisms, in general, have developed a mechanism by which some of their proteins, needed to cope with the new environmental conditions, undergo intracellular dislocalization (*86*−*88*). Given this scenario, the results of our experiment indicating a clear dislocation of LdCyP from the ER to the cytoplasm in the stress-induced cells with a concomitant increase in the specific activity of cytosolic AdK and facilitated intracellular AMP synthesis provided a compelling reason to believe that LdCyP−AdK interaction observed under *in vitro* condition is an *in vivo* reality and not simply a test tube curiosity. Several independent observations are consistent with this conclusion. First, despite the demonstrated nonessentiality of AdK in the promastigotes, hardly any data exist to suggest that its presence is also irrelevant for the survival of the amastigotes in the macrophage (*89*). On the contrary, like many other developmentally regulated parasitic proteins, AdK, along with adenosine deaminase (ADA), exhibits a higher level of activity during transformation from promastigote to amastigote with concomitant rapid utilization of Ado (*21*, *42*). Second, it is well established that promastigotes, upon exposure to elevated temperatures or other environmental stress, behave more like intracellular amastigotes (*19*, *37*, *39*). Third, during the transformation from promastigotes to amastigotes, the parasite is exposed to hostile conditions of the host macrophage, consisting of acidic pH, high temperature, and oxidative stress (*20*), and finally the sec61 translocon complex, responsible for both forward and retrograde transport of proteins across the ER membrane, is constituted of lumenal CyP as one of its components (*64*, *90*, *91*). In this connection it needs to be mentioned that, unlike many other strongly anchored ER-resident proteins, LdCyP lacks the ER anchoring sequence (KDEL). Therefore, there is a distinct possibility that stress may increase chances of its discharge into the cytosol using the sec61p channel complex tunnel. However, the detailed mechanism of such retrograde translocation, which is still a poorly understood phenomenon, will need further thorough investigation.

Why is the increased activity of AdK needed for the survival of the intracellular parasite? It is well established that AdK, in conjunction with ADA, plays a significant role in controlling *in vivo* Ado concentration (*92*). However, the pathways by which *L. donovani* assimilates Ado, as opposed to other purines, in its two morphological forms are different (*21*). In promastigotes, Ado is either cleaved to adenine by nucleosidase, an enzyme absent in amastigotes, or can be weakly phosphorylated to AMP by AdK, whereas amastigotes efficiently convert Ado to either AMP or inosine using respectively AdK and ADA, an enzyme totally absent in the promastigote (*21*). Therefore, to survive and multiply in the nondividing macrophages, the purine auxotrophic parasites need to scavenge purines or their corresponding riboside bases from the host nucleotide pool, comprised of adenylate as the most predominant nucleotide in all cells studied so far, with higher efficiency, thereby requiring the necessity of elevated levels of activity of both enzymes.

In conclusion, we have studied the mechanism of interaction of LdCyP with AdK, leading to its reactivation. In the process, a single positively charged residue, R147, of LdCyP has been identified as the nucleus of binding with AdK. Furthermore, the demonstration that ER-located LdCyP can indeed adopt a retrograde pathway for its transport into the cytoplasm, in addition to elucidating the physiological significance of the binding in the life cycle of the parasite, has opened a new opportunity to undertake detailed studies on the mechanism of retrograde translocation of proteins in the parasite. Gene knockout experiments and identification of other physiological partners of this ER-located LdCyP in this organism, naturally deficient in cytoplasmic CsA-binding activity, will facilitate such studies.

ACKNOWLEDGMENT

The authors thank Dr. Subrata Adak for critical help and Mr. Susanta Ghosh for technical assistance. All of the authors gratefully appreciate the help of Dr. Faye M. Johnson of the Thoracic Head and Neck Medical Oncology Department of M. D. Anderson Cancer Center, Houston, TX, for extending help in carrying out protein sequencing.

REFERENCES

1. Lodish, H. F., and Kong, N. (1991) Cyclosporin A inhibits an initial step in folding of transferrin within the endoplasmic reticulum, *J. Biol. Chem. 266*, 14835−14838.
2. Price, E. R., Zydowsky, L. D., Jin, M. J., Baker, C. H., McKeon, F. D., and Walsh, C. T. (1991) Human cyclophilin B: a second cyclophilin gene encodes a peptidyl-prolyl isomerase with a signal sequence, *Proc. Natl. Acad. Sci. U.S.A. 88*, 1903−1907.
3. Lilie, H., Lang, K., Rudolph, R., and Buchner, J. (1993) Prolyl isomerases catalyze antibody folding *in vitro*, *Protein Sci. 2*, 1490−1496.
4. Baker, E. K., Colley, N. J., and Zuker, C. S. (1994) The cyclophilin homolog NinaA functions as a chaperone, forming a stable complex *in vivo* with its protein target rhodopsin, *EMBO J. 13*, 4886−4895.
5. Rassow, J., Mohrs, K., Koidl, S., Barthelmess, I. B., Pfanner, N., and Tropschug, M. (1995) Cyclophilin 20 is involved in mitochondrial protein folding in cooperation with molecular chaperones Hsp70 and Hsp60, *Mol. Cell. Biol. 15*, 2654−2662.
6. Ferreira, P. A., Nakayama, T. A., Pak, W. L., and Travis, G. H. (1996) Cyclophilin-related protein RanBP2 acts as chaperone for red/green opsin, *Nature 383*, 637−640.
7. Braaten, D., and Luban, J. (2001) Cyclophilin A regulates HIV-1 infectivity, as demonstrated by gene targeting in human T cells, *EMBO J. 20*, 1300−1309.
8. Freskgard, P. O., Bergenhem, N., Jonsson, B. H., Svensson, M., and Carlsson, U. (1992) Isomerase and chaperone activity of prolyl isomerase in the folding of carbonic anhydrase, *Science 258*, 466−468.

9. Shieh, B. H., Stamnes, M. A., Seavello, S., Harris, G. L., and Zuker, C. S. (1989) The ninaA gene required for visual transduction in *Drosophila* encodes a homologue of cyclosporin A-binding protein, *Nature 338*, 67−70.
10. Luban, J., Bossolt, K. L., Franke, E. K., Kalpana, G. V., and Goff, S. P. (1993) Human immunodeficiency virus type 1 Gag protein binds to cyclophilins A and B, *Cell 73*, 1067−1078.
11. Lee, S. P., Hwang, Y. S., Kim, Y. J., Kwon, K. S., Kim, H. J., Kim, K., and Chae, H. Z. (2001) Cyclophilin A binds to peroxiredoxins and activates its peroxidase activity, *J. Biol. Chem. 276*, 29826−29832.
12. Jaschke, A., Mi, H., and Tropschug, M. (1998) Human T cell cyclophilin18 binds to thiol-specific antioxidant protein Aop1 and stimulates its activity, *J. Mol. Biol. 277*, 763−769.
13. Nadeau, K., Das, A., and Walsh, C. T. (1993) Hsp90 chaperonins possess ATPase activity and bind heat shock transcription factors and peptidyl prolyl isomerases, *J. Biol. Chem. 268*, 1479−1487.
14. Carrello, A., Allan, R. K., Morgan, S. L., Owen, B. A., Mok, D., Ward, B. K., Minchin, R. F., Toft, D. O., and Ratajczak, T. (2004) Interaction of the Hsp90 cochaperone cyclophilin 40 with Hsc70, *Cell Stress Chaperones 9*, 167−181.
15. Ou, W. B., Luo, W., Park, Y. D., and Zhou, H. M. (2001) Chaperone-like activity of peptidyl-prolyl cis-trans isomerase during creatine kinase refolding, *Protein Sci. 10*, 2346−2353.
16. Furutani, M., Ideno, A., Iida, T., and Maruyama, T. (2000) FK506 binding protein from a thermophilic archaeon, *Methanococcus thermolithotrophicus*, has chaperone-like activity *in vitro*, *Biochemistry 39*, 453−462.
17. Bergsma, D. J., Eder, C., Gross, M., Kersten, H., Sylvester, D., Appelbaum, E., Cusimano, D., Livi, G. P., McLaughlin, M. M., Kasyan, K., et al. (1991) The cyclophilin multigene family of peptidyl-prolyl isomerases. Characterization of three separate human isoforms, *J. Biol. Chem. 266*, 23204−23214.
18. Chang, K. P. (1979) *Leishmania donovani*: promastigote−macrophage surface interactions *in vitro*, *Exp. Parasitol. 48*, 175−189.
19. Argaman, M., Aly, R., and Shapira, M. (1994) Expression of heat shock protein 83 in *Leishmania* is regulated post-transcriptionally, *Mol. Biochem. Parasitol. 64*, 95−110.
20. Bente, M., Harder, S., Wiesgigl, M., Heukeshoven, J., Gelhaus, C., Krause, E., Clos, J., and Bruchhaus, I. (2003) Developmentally induced changes of the proteome in the protozoan parasite *Leishmania donovani*, *Proteomics 3*, 1811−1829.
21. Looker, D. L., Berens, R. L., and Marr, J. J. (1983) Purine metabolism in *Leishmania donovani* amastigotes and promastigotes, *Mol. Biochem. Parasitol. 9*, 15−28.
22. Ratajczak, T., Carrello, A., Mark, P. J., Warner, B. J., Simpson, R. J., Moritz, R. L., and House, A. K. (1993) The cyclophilin component of the unactivated estrogen receptor contains a tetratricopeptide repeat domain and shares identity with p59 (FKBP59), *J. Biol. Chem. 268*, 13187−13192.
23. Sen, B., Chakraborty, A., Datta, R., Bhattacharyya, D., and Datta, A. K. (2006) Reversal of ADP-mediated aggregation of adenosine kinase by cyclophilin leads to its reactivation, *Biochemistry 45*, 263−271.
24. Chakraborty, A., Das, I., Datta, R., Sen, B., Bhattacharyya, D., Mandal, C., and Datta, A. K. (2002) A single-domain cyclophilin from *Leishmania donovani* reactivates soluble aggregates of adenosine kinase by isomerase-independent chaperone function, *J. Biol. Chem. 277*, 47451−47460.
25. Chakraborty, A., Sen, B., Datta, R., and Datta, A. K. (2004) Isomerase-independent chaperone function of cyclophilin ensures aggregation prevention of adenosine kinase both *in vitro* and under *in vivo* conditions, *Biochemistry 43*, 11862−11872.
26. Rotonda, J., Burbaum, J. J., Chan, H. K., Marcy, A. I., and Becker, J. W. (1993) Improved calcineurin inhibition by yeast FKBP12-drug complexes. Crystallographic and functional analysis, *J. Biol. Chem. 268*, 7607−7609.
27. Patzelt, H., Rudiger, S., Brehmer, D., Kramer, G., Vorderwulbecke, S., Schaffitzel, E., Waitz, A., Hesterkamp, T., Dong, L., Schneider-Mergener, J., Bukau, B., and Deuerling, E. (2001) Binding specificity of *Escherichia coli* trigger factor, *Proc. Natl. Acad. Sci. U.S.A. 98*, 14244−14249.
28. Pak, M., and Wickner, S. (1997) Mechanism of protein remodeling by ClpA chaperone, *Proc. Natl. Acad. Sci. U.S.A. 94*, 4901−4906.
29. Nicholls, A., Sharp, K. A., and Honig, B. (1991) Protein folding and association: insights from the interfacial and thermodynamic properties of hydrocarbons, *Proteins 11*, 281−296.
30. Xu, W., Yuan, X., Xiang, Z., Mimnaugh, E., Marcu, M., and Neckers, L. (2005) Surface charge and hydrophobicity determine ErbB2 binding to the Hsp90 chaperone complex, *Nat. Struct. Mol. Biol. 12*, 120−126.
31. Friedman, J., Trahey, M., and Weissman, I. (1993) Cloning and characterization of cyclophilin C-associated protein: a candidate natural cellular ligand for cyclophilin C, *Proc. Natl. Acad. Sci. U.S.A. 90*, 6815−6819.
32. Dutta, M., Delhi, P., Sinha, K. M., Banerjee, R., and Datta, A. K. (2001) Lack of abundance of cytoplasmic cyclosporin A-binding protein renders free-living *Leishmania donovani* resistant to cyclosporin A, *J. Biol. Chem. 276*, 19294−19300.
33. Ke, H., Zhao, Y., Luo, F., Weissman, I., and Friedman, J. (1993) Crystal structure of murine cyclophilin C complexed with immunosuppressive drug cyclosporin A, *Proc. Natl. Acad. Sci. U.S.A. 90*, 11850−11854.
34. Sinha, K. M., Ghosh, M., Das, I., and Datta, A. K. (1999) Molecular cloning and expression of adenosine kinase from *Leishmania donovani*: identification of unconventional P-loop motif, *Biochem. J. 339* (Part 3), 667−673.
35. Bhaumik, D., and Datta, A. K. (1989) Immunochemical and catalytic characteristics of adenosine kinase from *Leishmania donovani*, *J. Biol. Chem. 264*, 4356−4361.
36. Datta, A. K., Bhaumik, D., and Chatterjee, R. (1987) Isolation and characterization of adenosine kinase from *Leishmania donovani*, *J. Biol. Chem. 262*, 5515−5521.
37. Saar, Y., Ransford, A., Waldman, E., Mazareb, S., Amin-Spector, S., Plumblee, J., Turco, S. J., and Zilberstein, D. (1998) Characterization of developmentally-regulated activities in axenic amastigotes of *Leishmania donovani*, *Mol. Biochem. Parasitol. 95*, 9−20.
38. Miller, M. A., McGowan, S. E., Gantt, K. R., Champion, M., Novick, S. L., Andersen, K. A., Bacchi, C. J., Yarlett, N., Britigan, B. E., and Wilson, M. E. (2000) Inducible resistance to oxidant stress in the protozoan *Leishmania chagasi*, *J. Biol. Chem. 275*, 33883−33889.
39. Wiesgigl, M., and Clos, J. (2001) Heat shock protein 90 homeostasis controls stage differentiation in *Leishmania donovani*, *Mol. Biol. Cell 12*, 3307−3316.
40. Toner, J. J., and Weber, M. M. (1972) Respiratory control in mitochondria from *Crithidia fasciculata*, *Biochem. Biophys. Res. Commun. 46*, 652−660.
41. Sarkar, M., Hamilton, C. J., and Fairlamb, A. H. (2003) Properties of phosphoenolpyruvate mutase, the first enzyme in the aminoethylphosphonate biosynthetic pathway in *Trypanosoma cruzi*, *J. Biol. Chem. 278*, 22703−22708.
42. Iovannisci, D. M., and Ullman, B. (1984) Characterization of a mutant *Leishmania donovani* deficient in adenosine kinase activity, *Mol. Biochem. Parasitol. 12*, 139−151.
43. Zarley, J. H., Britigan, B. E., and Wilson, M. E. (1991) Hydrogen peroxide-mediated toxicity for *Leishmania donovani chagasi* promastigotes. Role of hydroxyl radical and protection by heat shock, *J. Clin. Invest. 88*, 1511−1521.
44. Banerjee, R., Dutta, M., Sen, M., and Datta, A. K. (2002) Crystallization and preliminary X-ray analysis of cyclophilin from *Leishmania donovani*, *Acta Crystallogr., Sect. D: Biol. Crystallogr. 58*, 1846−1847.
45. Navaza, J. (1994) AmoRe: an automated package for molecular replacement, *Acta Crystallogr. A50*, 157−163.
46. Jones, T. A., Zou, J. Y., Cowan, S. W., and Kjeldgaard (1991) Improved methods for building protein models in electron density maps and the location of errors in these models, *Acta Crystallogr A47* (Part 2), 110−119.
47. Brunger, A. T., Adams, P. D., Clore, G. M., DeLano, W. L., Gros, P., Grosse-Kunstleve, R. W., Jiang, J. S., Kuszewski, J., Nilges, M., Pannu, N. S., Read, R. J., Rice, L. M., Simonson, T., and Warren, G. L. (1998) Crystallography & NMR system: A new software suite for macromolecular structure determination, *Acta Crystallogr., Sect. D: Biol. Crystallogr. 54*, 905−921.
48. Laskowski, R. A., MacArthur, M. W., Moss, D. S., and Thornton, J. M. (1993) PROCHECK: a program to check the stereochemical quality of protein structures, *J. Appl. Crystallogr. 26*, 283−291.
49. Sali, A., and Blundell, T. L. (1993) Comparative protein modelling by satisfaction of spatial restraints, *J. Mol. Biol. 234*, 779−815.
50. Richards, F. M. (1974) The interpretation of protein structures: total volume, group volume distributions and packing density, *J. Mol. Biol. 82*, 1−14.
51. Banerjee, R., Sen, M., Bhattacharya, D., and Saha, P. (2003) The jigsaw puzzle model: search for conformational specificity in protein interiors, *J. Mol. Biol. 333*, 211−226.

52. Wang, X., Ching, Y. P., Lam, W. H., Qi, Z., Zhang, M., and Wang, J. H. (2000) Identification of a common protein association region in the neuronal Cdk5 activator, *J. Biol. Chem. 275*, 31763−31769.
53. Tan, Y. J., and Ting, A. E. (2000) Non-ionic detergent affects the conformation of a functionally active mutant of Bcl-X(L), *Protein Eng. 13*, 887−892.
54. Hicks, S. N., Smiley, R. D., Hamilton, J. B., and Howell, E. E. (2003) Role of ionic interactions in ligand binding and catalysis of R67 dihydrofolate reductase, *Biochemistry 42*, 10569−10578.
55. Schlarb-Ridley, B. G., Bendall, D. S., and Howe, C. J. (2002) Role of electrostatics in the interaction between cytochrome *f* and plastocyanin of the cyanobacterium *Phormidium laminosum*, *Biochemistry 41*, 3279−3285.
56. Xu, D., Lin, S. L., and Nussinov, R. (1997) Protein binding versus protein folding: the role of hydrophilic bridges in protein associations, *J. Mol. Biol. 265*, 68−84.
57. Weisman, R., Creanor, J., and Fantes, P. (1996) A multicopy suppressor of a cell cycle defect in *S. pombe* encodes a heat shock-inducible 40 kDa cyclophilin-like protein, *EMBO J. 15*, 447−456.
58. Sykes, K., Gething, M. J., and Sambrook, J. (1993) Proline isomerases function during heat shock, *Proc. Natl. Acad. Sci. U.S.A. 90*, 5853−5857.
59. Andreeva, L., Motterlini, R., and Green, C. J. (1997) Cyclophilins are induced by hypoxia and heat stress in myogenic cells, *Biochem. Biophys. Res. Commun. 237*, 6−9.
60. Chang, K. P., and Dwyer, D. M. (1976) Multiplication of a human parasite (*Leishmania donovani*) in phagolysosomes of hamster macrophages *in vitro*, *Science 193*, 678−680.
61. Debrabant, A., Lee, N., Pogue, G. P., Dwyer, D. M., and Nakhasi, H. L. (2002) Expression of calreticulin P-domain results in impairment of secretory pathway in *Leishmania donovani* and reduced parasite survival in macrophages, *Int. J. Parasitol. 32*, 1423−1434.
62. Ye, Y., Shibata, Y., Yun, C., Ron, D., and Rapoport, T. A. (2004) A membrane protein complex mediates retro-translocation from the ER lumen into the cytosol, *Nature 429*, 841−847.
63. VanSlyke, J. K., and Musil, L. S. (2002) Dislocation and degradation from the ER are regulated by cytosolic stress, *J. Cell Biol. 157*, 381−394.
64. Romisch, K. (1999) Surfing the Sec61 channel: bidirectional protein translocation across the ER membrane, *J. Cell Sci. 112* (Part 23), 4185−4191.
65. Tirosh, B., Furman, M. H., Tortorella, D., and Ploegh, H. L. (2003) Protein unfolding is not a prerequisite for endoplasmic reticulum-to-cytosol dislocation, *J. Biol. Chem. 278*, 6664−6672.
66. Holmsen, H., and Rozenberg, M. C. (1968) Adenine nucleotide metabolism of blood platelets. I. Adenosine kinase and nucleotide formation from exogenous adenosine and AMP, *Biochim. Biophys. Acta 155*, 326−341.
67. Parks, R. E., Jr., and Brown, P. R. (1973) Incorporation of nucleosides into the nucleotide pools of human erythrocytes. Adenosine and its analogs, *Biochemistry 12*, 3294−3302.
68. Schrader, J., Berne, R. M., and Rubio, R. (1972) Uptake and metabolism of adenosine by human erythrocyte ghosts, *Am. J. Physiol. 223*, 159−166.
69. Buchner, J. (1996) Supervising the fold: functional principles of molecular chaperones, *FASEB J. 10*, 10−19.
70. Harding, M. W., Handschumacher, R. E., and Speicher, D. W. (1986) Isolation and amino acid sequence of cyclophilin, *J. Biol. Chem. 261*, 8547−8555.
71. Yarovinsky, F., Andersen, J. F., King, L. R., Caspar, P., Aliberti, J., Golding, H., and Sher, A. (2004) Structural determinants of the anti-HIV activity of a CCR5 antagonist derived from *Toxoplasma gondii*, *J. Biol. Chem. 279*, 53635−53642.
72. Holm, M., Hardtke, C. S., Gaudet, R., and Deng, X. W. (2001) Identification of a structural motif that confers specific interaction with the WD40 repeat domain of *Arabidopsis* COP1, *EMBO J. 20*, 118−127.
73. Hase, M., Yoshimi, T., Ishikawa, Y., Ohba, A., Guo, L., Mima, S., Makise, M., Yamaguchi, Y., Tsuchiya, T., and Mizushima, T. (1998) Site-directed mutational analysis for the membrane binding of DnaA protein. Identification of amino acids involved in the functional interaction between DnaA protein and acidic phospholipids, *J. Biol. Chem. 273*, 28651−28656.
74. Schedin-Weiss, S., Desai, U. R., Bock, S. C., Olson, S. T., and Bjork, I. (2004) Roles of N-terminal region residues Lys11, Arg13, and Arg24 of antithrombin in heparin recognition and in promotion and stabilization of the heparin-induced conformational change, *Biochemistry 43*, 675−683.
75. Teigelkamp, S., Achsel, T., Mundt, C., Gothel, S. F., Cronshagen, U., Lane, W. S., Marahiel, M., and Luhrmann, R. (1998) The 20kD protein of human [U4/U6.U5] tri-snRNPs is a novel cyclophilin that forms a complex with the U4/U6-specific 60kD and 90kD proteins, *RNA 4*, 127−141.
76. Kim, S. Y., Semyonov, A. N., Twieg, R. J., Horwich, A. L., Frydman, J., and Moerner, W. E. (2005) Probing the sequence of conformationally induced polarity changes in the molecular chaperonin GroEL with fluorescence spectroscopy, *J. Phys. Chem. B 109*, 24517−24525.
77. Jewett, A. I., Baumketner, A., and Shea, J. E. (2004) Accelerated folding in the weak hydrophobic environment of a chaperonin cavity: creation of an alternate fast folding pathway, *Proc. Natl. Acad. Sci. U.S.A. 101*, 13192−13197.
78. Steinbacher, S. (1999) Crystal structure of the post-chaperonin beta-tubulin binding cofactor Rbl2p, *Nat. Struct. Biol. 6*, 1029−1032.
79. Pace, C. N., Shirley, B. A., McNutt, M., and Gajiwala, K. (1996) Forces contributing to the conformational stability of proteins, *FASEB J. 10*, 75−83.
80. Hurley, J. K., Hazzard, J. T., Martinez-Julvez, M., Medina, M., Gomez-Moreno, C., and Tollin, G. (1999) Electrostatic forces involved in orienting *Anabaena* ferredoxin during binding to *Anabaena* ferredoxin:$NADP^+$ reductase: site-specific mutagenesis, transient kinetic measurements, and electrostatic surface potentials, *Protein Sci. 8*, 1614−1622.
81. Braun, W., Kallen, J., Mikol, V., Walkinshaw, M. D., and Wuthrich, K. (1995) Three-dimensional structure and actions of immunosuppressants and their immunophilins, *FASEB J. 9*, 63−72.
82. Golding, H., Aliberti, J., King, L. R., Manischewitz, J., Andersen, J., Valenzuela, J., Landau, N. R., and Sher, A. (2003) Inhibition of HIV-1 infection by a CCR5-binding cyclophilin from *Toxoplasma gondii*, *Blood 102*, 3280−3286.
83. Mikol, V., Kallen, J., and Walkinshaw, M. D. (1994) X-ray structure of a cyclophilin B/cyclosporin complex: comparison with cyclophilin A and delineation of its calcineurin-binding domain, *Proc. Natl. Acad. Sci. U.S.A. 91*, 5183−5186.
84. Halestrap, A. P., Woodfield, K. Y., and Connern, C. P. (1997) Oxidative stress, thiol reagents, and membrane potential modulate the mitochondrial permeability transition by affecting nucleotide binding to the adenine nucleotide translocase, *J. Biol. Chem. 272*, 3346−3354.
85. Temkin, V., Huang, Q., Liu, H., Osada, H., and Pope, R. M. (2006) Inhibition of ADP/ATP exchange in receptor-interacting protein-mediated necrosis, *Mol. Cell. Biol. 26*, 2215−2225.
86. Wood, M. J., Storz, G., and Tjandra, N. (2004) Structural basis for redox regulation of Yap1 transcription factor localization, *Nature 430*, 917−921.
87. Tortorella, D., Story, C. M., Huppa, J. B., Wiertz, E. J., Jones, T. R., Bacik, I., Bennink, J. R., Yewdell, J. W., and Ploegh, H. L. (1998) Dislocation of type I membrane proteins from the ER to the cytosol is sensitive to changes in redox potential, *J. Cell Biol. 142*, 365−376.
88. Ledesma, M. D., Galvan, C., Hellias, B., Dotti, C., and Jensen, P. H. (2002) Astrocytic but not neuronal increased expression and redistribution of parkin during unfolded protein stress, *J. Neurochem. 83*, 1431−1440.
89. Hwang, H. Y., and Ullman, B. (1997) Genetic analysis of purine metabolism in *Leishmania donovani*, *J. Biol. Chem. 272*, 19488−19496.
90. Smith, T., Ferreira, L. R., Hebert, C., Norris, K., and Sauk, J. J. (1995) Hsp47 and cyclophilin B traverse the endoplasmic reticulum with procollagen into pre-Golgi intermediate vesicles. A role for Hsp47 and cyclophilin B in the export of procollagen from the endoplasmic reticulum, *J. Biol. Chem. 270*, 18323−18328.
91. Meunier, L., Usherwood, Y. K., Chung, K. T., and Hendershot, L. M. (2002) A subset of chaperones and folding enzymes form multiprotein complexes in endoplasmic reticulum to bind nascent proteins, *Mol. Biol. Cell 13*, 4456−4469.
92. Berne, R. M., Knabb, R. M., Ely, S. W., and Rubio, R. (1983) Adenosine in the local regulation of blood flow: a brief overview, *Fed. Proc. 42*, 3136−3142.

BI602625H